Optical phonon–assisted magnetotunneling peaks in GaAs/$Al_xGa_{1-x}As$ double-barrier structures

Zu Wei Yan[1,2,3,*] and X. X. Liang[1,2,†]
[1]*CCAST (World Laboratory), P.O. Box 8730, Beijing 100080, People's Republic of China*
[2]*Department of Physics, Inner Mongolia University, Hohhot 010021, People's Republic of China*[‡]
[3]*Department of Basic Sciences, Inner Mongolia Agricultural University, Hohhot 010018, People's Republic of China*
(Received 27 June 2002; published 31 December 2002)

The effect of the interface optical (IO) phonons and the confined LO phonons in a $Al_xGa_{1-x}As$ emitter barrier and GaAs quantum well on the phonon-assisted tunneling through a double-barrier structure has been studied in the presence of a magnetic field in the direction of the current. The tunneling current densities are calculated and the numerical results for the typical GaAs/$Al_xGa_{1-x}As$ structures are given graphically. An alternative recognition of the phonon-assisted tunneling current peaks is suggested. Only one theoretical peak from the IO phonons and the confined LO phonons is easy to be observed for wide well systems. The second peak appears at the position corresponding to the emission of the confined higher-frequency branch LO phonon in the ternary mixed-crystal emitter barrier and can also be observed in the narrower-well systems.

DOI: 10.1103/PhysRevB.66.235324 PACS number(s): 73.40.Gk, 72.10.Di, 63.20.Kr

I. INTRODUCTION

Optical phonon–assisted tunneling (PAT) in a double-barrier structure (DBS) has attracted a great deal of experimental[1–3] and theoretical[4–10] interest over the past few years. The satellite peaks subjected to the PAT have been experimentally observed in the valley current region at low temperatures.[1–3] The PAT experiments in the presence of a magnetic field parallel to the electric current found that the satellite peaks become higher and sharper with increasing magnetic field, and also split into several peaks associated with the transitions between the Landau levels of the emitter and well layers.[2,3] Early theoretical works calculated PAT currents in DBSs and explained the satellite peaks by the emission of longitudinal optical (LO) phonons.[4,5] Further investigations[6,11–13] indicated that the IO-phonon modes play an important role in the electron-phonon (*e*-ph) interaction properties in multilayer systems and also in the PAT currents in DBSs. Moreover, the experimental observations displayed the characteristic that only one PAT peak can be observed for wide well systems, and the ''second peak'' appears in the narrow-well case.[2,3] Unfortunately, the phenomena have not been explained satisfactorily by theoretical calculations, to our knowledge.

Recent theoretical studies on the PAT in an asymmetric DBS[9,10] show that PAT peaks from both IO phonons and confined LO phonons occur at the same site corresponding to the bulk GaAs LO-phonon frequency, and the IO-phonon contributions are more significant than that from the confined LO phonon in the well. The PAT peaks become higher and sharper with increasing magnetic field. However, the effect of LO phonons confined in the emitter barrier or the collector barrier on the PAT current have not been discussed in detail in the previous theoretical calculations. In fact, the electronic incident wave penetrates first into the emitter barrier, so that the confined LO phonons in the barrier must be excited and assist the PAT, particularly in the narrow-well case. We might guess if the second peak is subject to the emitter barrier LO phonons. To this end, a detailed theoretical recognition of the PAT peaks in DBSs is invoked.

As is well known, the optical frequencies exhibit two-mode behavior in a ternary mixed crystal (TMC).[14–18] The confined LO phonons with two different frequencies in the barriers of TMC $Al_xGa_{1-x}As$ both couple with the electron and contribute to the PAT current. However, to our knowledge, few theoretical calculations for the PAT current have mentioned the two branches of TMC LO-phonon modes. Therefore a more detailed theoretical treatment, including the effect of confined barrier LO phonons as well as well LO phonons and IO phonons, is necessary to understand the roles of the two branches of LO-phonon modes of the TMC $Al_xGa_{1-x}As$ barrier.

In this paper, we study theoretically phonon-assisted magnetotunneling (PAMT) processes in a DBS. The contributions of the two branches of LO phonons confined in the $Al_xGa_{1-x}As$ emitter barrier to PAMT are both included in the calculations, besides the confined well LO phonons and IO phonons. The PAMT current is calculated by using the Fermi golden rule. The numerical computations for the confined barrier and well LO- and IO-phonon-assisted currents in the GaAs/$Al_xGa_{1-x}As$ DBS are performed for different external magnetic filed. The result shows that the second PAMT peak corresponding to the emission of confined emitter barrier phonons can be also observed for narrower wells.

II. THEORY

Consider a DBS composed of the GaAs and $Al_xGa_{1-x}As$ material layers alternately. The five layers of polar crystal materials lie in region I ($z<-d_2-d_3/2$), II ($-d_2-d_3/2 \leqslant z<-d_3/2$), III ($-d_3/2\leqslant z<d_3/2$), IV ($d_3/2\leqslant z<d_4+d_3/2$), and V ($z\geqslant d_4+d_3/2$), respectively. An electric field and a magnetic field are applied along the growth direction of the DBS, i.e., the z axis. A beam of electrons of effective mass m_j^* is emitted into the system with kinetic energy E. To calculate the PAMT current, we write down the Hamiltonian of the *e*-ph system with the external electric and magnetic fields

$$H=H_e+H_{\rm ph}+H_{e\text{-ph}}. \tag{1}$$

The first term in Eq. (1) is the electronic Hamiltonian and given by

$$H_e=\frac{1}{2m_j^*}[(p_x-eBy)^2+p_y^2+p_z^2]+U_j(z). \tag{2}$$

Here we have chosen the Landau gauge for the vector potential $\vec{A}$ describing the applied magnetic field $\vec{B}$, i.e., $\vec{A}=(-By,0,0)$. $U_j(z)$ is the potential undergone by the electron, including both the effects of conduction-band discontinuities at GaAs/Al_xGa_{1-x}As (Ref. 19) interfaces and external applied voltage. The second term is the free-phonon field Hamiltonian and has the well-known form

$$H_{\rm ph}=\sum_{\vec{q}jm}\hbar\omega_{Lj}a^{\dagger}_{\vec{q}jm}a_{\vec{q}jm}+\sum_{\vec{q}\nu}\hbar\omega_{I\nu}a^{\dagger}_{\vec{q}\nu}a_{\vec{q}\nu}. \tag{3}$$

Here $\hbar\omega_{Lj}$ and $\hbar\omega_{I\nu}$ are, respectively, the frequencies of LO and IO phonons, and j and ν are the corresponding branch indexes of phonon modes. The third term in Eq. (1), the *e*-ph interaction term, can be written as

$$H_{e\text{-ph}}=H_{e\text{-}Leb}+H_{e\text{-}Lcb}+H_{e\text{-}Lw}+H_{e\text{-}I}, \tag{4}$$

where $H_{e\text{-}I}$ and $H_{e\text{-}Lw}$ describe, respectively, the electron–IO-phonon (e–IO–ph) interaction and the interaction between the electron and the well phonon modes, and given in previous references.[9,10,12] $H_{e\text{-}Leb}$, and $H_{e\text{-}Lcb}$ are, respectively, the interactions between the electron and the confined LO phonons in the emitter and collector barriers. Within the framework of the random-element-isodisplacement model[14] and the continuum dielectric model,[16,17] the *e*-ph interaction Hamiltonian subjected to the emitter barrier LO phonons, $H_{e\text{-}Leb}$, can be written as the following form:[13,18]

$$H_{e\text{-}Leb}=\sum_{\vec{q}lm}\frac{1}{\sqrt{S}}\beta_{lm}(q)\times\left\{\begin{array}{c}\cos\dfrac{(2m-1)\pi}{d_2}\left(z+\dfrac{d_2+d_3}{2}\right)\\ \sin\dfrac{2m\pi}{d_2}\left(z+\dfrac{d_2+d_3}{2}\right)\end{array}\right\}$$
$$\times e^{i\vec{q}\cdot\vec{\rho}}a_{\vec{q}lm}+hc,\quad m=1,2,3,\ldots. \tag{5}$$

In Eq. (5), $a^{\dagger}_{\vec{q}lm}$ and $a_{\vec{q}lm}$ are the creation and annihilation operators of emitter barrier LO phonons with the frequency ω_{lL}, where $l=1$ and 2 stand for the higher- and lower-frequency branches of the LO-phonon modes of the mixed crystal $Al_xGa_{1-x}As$, respectively. S is the area of the interfaces, $\vec{q}$ and $\vec{\rho}$ are, respectively, the two-dimensional wave vector and position vector in the x-y plane. The coupling function in Eq. (5) are given by

$$\beta_{lm}(q)=\left(\frac{2g_l^2}{d_2}\right)^{1/2}\left(q^2+\frac{m^2\pi^2}{d_2^2}\right)^{-1/2}, \tag{6}$$

where

$$g_1=\frac{ie}{\varepsilon_0+b_{33}}\left(\frac{\hbar}{2\omega_{1L}}\right)^{1/2}\left[\frac{1}{T_{11}+2B_1T_{12}+B_1^2T_{22}}\right]^{1/2}$$
$$\times(b_{31}+B_1b_{32}), \tag{7a}$$

$$g_2=\frac{ie}{\varepsilon_0+b_{33}}\left(\frac{\hbar}{2\omega_{2L}}\right)^{1/2}\left[\frac{1}{T_{11}+2B_2T_{12}+B_{21}^2T_{22}}\right]^{1/2}$$
$$\times(b_{31}+B_2b_{32}), \tag{7b}$$

with

$$T_{11}=\frac{m_Ax[m_C+m_B(1-x)]}{\mu_AM},$$

$$T_{12}=T_{21}=-\frac{m_Axm_B(1-x)}{\sqrt{\mu_A\mu_B}M},$$

$$T_{22}=\frac{m_B(1-x)[m_C+m_Ax]}{\mu_BM}, \tag{8a}$$

$$B_1=-\frac{T_{12}b'_{21}+T_{11}(b'_{11}+\omega_{1L}^2)}{T_{11}b'_{12}+T_{12}(b'_{22}+\omega_{1L}^2)},$$

$$B_2=-\frac{T_{12}b'_{21}+T_{11}(b'_{11}+\omega_{2L}^2)}{T_{11}b'_{12}+T_{12}(b'_{22}+\omega_{2L}^2)}, \tag{8b}$$

ω_{lL} is given by

$$\omega_{lL}^2=\{-(b'_{11}+b'_{22})\pm[(b'_{11}-b'_{22})^2+4b'_{12}b'_{21}]^{1/2}\}/2, \tag{8c}$$

where the sign + (−) corresponds to the higher- (lower-) frequency branch, i.e., $l=1$ (2), and

$$b'_{ij}=b_{ij}-b_{i3}b_{3j}/(\varepsilon_0+b_{33}),\quad i,j=1,2. \tag{9}$$

The dynamic coefficients b_{ij} $(i,j=1,2,3)$ and related parameters are given and the meanings of the parameters mentioned in the equations are well known, as in Ref. 17. The interaction Hamiltonian between the electron and the collector barrier LO phonons, $H_{e\text{-}Lcb}$, has the same form as that of $H_{e\text{-}Leb}$ given by Eq. (5).

To calculate the PAMT, we use the effective-mass approximation and assume the DBS potential-energy function invariant. The initial (before tunneling) and final (after tunneling) electronic wave functions are chosen as follows:

$$\psi_i(\vec{r})=\frac{e^{ik_xx}}{\sqrt{L_x}}\chi_i(y)\varphi_i(z), \tag{10}$$

$$\psi_f(\vec{r})=\frac{e^{ik'_xx}}{\sqrt{L_x}}\chi_f(y)\varphi_f(z), \tag{11}$$

where L_x and k_x are, respectively, the lengths of the device and the wave vector in the x direction. $\chi_i(y)$ and $\chi_f(y)$ are, respectively, the wave functions of the initial and final states of the electronic cyclotron motion in the x-y plane, whose eigenfunction corresponding to the nth Landau level is given by

$$\chi_n(y)=\left(\frac{\gamma}{2^n\sqrt{\pi}n!}\right)^{1/2}H_n(\gamma(y-y_0))e^{-(\gamma^2/2)(y-y_0)^2}. \tag{12}$$

Here $\gamma^{-1}=(m_j^*\omega_c/\hbar)^{-1/2}=(eB/\hbar)^{-1/2}$ is the cyclotron radius of $n=0$ and $\omega_c=eB/m_j^*$ the cyclotron frequency. H_n denotes the Hermite polynomial of order n, where $n=0,1,2,3,...$ refers to the Landau level and $y_0=\hbar k_x/eB$. The energies of the initial and final electronic states can then be written as

$$E_i=\hbar\omega_c(n_i+\tfrac{1}{2})+E_z, \quad E_f=\hbar\omega_c(n_f+\tfrac{1}{2})+E_{zf}, \quad (13)$$

where E_z and E_{zf} are the energies in the z direction. For PAMT processes, $\varphi_i(z)$ is a plane wave state, and $\varphi_f(z)$ the quasibound resonant wave function with energy E_{zf}.[5,6,19,20]

At the voltages above the resonant tunneling value, a small portion of the emitter electronic wave function extends into the DBS and couples with the quasibound resonant state though the emission of a optical phonon.[4–6,9,10] The phonon emission rates can be obtained by the Fermi golden rules

$$W^{i\to f}(\vec{k})=\frac{2\pi}{\hbar}|\langle f|H_{e\text{-ph}}|i\rangle|^2\,\delta(E_i-E_f-\hbar\omega(q)), \quad (14)$$

where $\hbar\omega(q)$ is the energy of the emitted phonon and $\vec{k}=(k_x,k_z)$ is the two-dimensional wave vector. The initial and final states are, respectively, the single-electronic states without and with emitted phonons given by

$$|i\rangle=|\psi_i\rangle|0_q\rangle, \quad |f\rangle=|\psi_f\rangle|1_q\rangle, \quad (15)$$

where $|0_q\rangle$ and $|1_q\rangle$ are, respectively, the zero-phonon and one-phonon states of wave vector q.

Inserting the Hamitonian (4) into Eq. (14) and integrating over all final states yields the phonon emission rate $W(\vec{k},V,n_i,n_f)$. Multiplying the number of electrons in a small region of two-dimensional $\vec{k}$ space by the phonon emission rate and integrating over $\vec{k}$, one can obtain the excess current density due to PAMT as

$$J(V,n_i,n_f)=\frac{e}{S}\int W(\vec{k},V,n_i,n_f)g(\vec{k})f(\vec{k})d\vec{k}, \quad (16)$$

where $f(\vec{k})$ and $g(\vec{k})=2L_xL_z/(2\pi)^2$ are, respectively, the Fermi function and the state density of the electrons of the n_ith Landau level in the emitter. In Eq. (16) we have confined our discussion to the low-temperature case so that the phonon absorption effect is neglected. It is also assumed that the tunneling current is so small that the electron-phonon system keeps in an equilibrium state. The upper limit of k_x in the integral is chosen as $k_{x\,\max}=eBL_y/\hbar$.

The PAMT current density assisted by the confined LO_{eb} phonons in the emitter barrier can be calculated by

$$J_{Leb}(V,n_i,n_f)=\frac{e^2Bm^{*1/2}L_z}{2^{3/2}\pi^3\hbar^3}\sum_{ml}\frac{f(E_z,B)}{\sqrt{E_z}}\frac{g_l^2}{d_2}|M_m^{eb}|^2\int_0^\infty dq_x \times\int_0^\infty dq_y\frac{|G(q,n_i,n_f)|^2}{q^2+(m\pi/d_2)^2}, \quad (17)$$

where $q^2=q_x^2+q_y^2$. M_m^{eb} and $G(q,n_i,n_f)$ are all the overlap integrals and are given by

$$M_m^{eb}=\int_{-\infty}^{\infty}\varphi_f^*(z)\times\left\{\begin{array}{c}\cos\dfrac{(2m-1)\pi}{d_2}\left(z+\dfrac{d_2+d_3}{2}\right)\\ \sin\dfrac{2m\pi}{d_2}\left(z+\dfrac{d_2+d_3}{2}\right)\end{array}\right\}\times\varphi_i(z)dz, \quad m=1,2,3.... \quad (18a)$$

$$G(q,n_i,n_f)=\int_{-\infty}^{\infty}\chi_f^*(y)e^{iq_yy}\chi_i(y)dy. \quad (18b)$$

In the equations, $E_z=E_{zf}-\hbar\omega_c(n_i-n_f)+\hbar\omega_{Leb}$ is the energy of incident electrons.

The LO_w-PAMT current density assisted by well phonons can be written as

$$J_{Lw}(V,n_i,n_f)=\frac{e^2Bm^{*1/2}L_z}{2^{5/2}\pi^3\hbar^3}\sum_m\frac{f(E_z,B)}{\sqrt{E_z}}\alpha^2|M_m^w|^2\int_0^\infty dq_x \times\int_0^\infty dq_y\frac{|G(q,n_i,n_f)|^2}{q^2+(m\pi/d_3)^2}, \quad (19)$$

with

$$\alpha=\left[\frac{e^2\hbar\omega_{Lw}}{\varepsilon_0 d_3}\left(\frac{1}{\varepsilon_{\infty 3}}-\frac{1}{\varepsilon_{03}}\right)\right]^{1/2}, \quad (20a)$$

$$M_m^w=\int_{-\infty}^{\infty}\varphi_f^*(z)\times\left\{\begin{array}{c}\cos\dfrac{(2m-1)\pi}{d_3}z\\ \sin\dfrac{2m\pi}{d_3}z\end{array}\right\}\times\varphi_i(z)dz, \quad m=1,2,3,.... \quad (20b)$$

At the long-wavelength limit, the IO-PAMT current density is then written as

$$J_I(V,n_i,n_f)=\frac{e^2Bm^{*1/2}L_z}{2^{5/2}\pi^3\hbar^3}\sum_\nu\frac{f(E_z,B)}{\sqrt{E_z}}\int_0^\infty dq_x \times\int_0^\infty dq_y\beta_\nu^2(q)|M(q)|^2|G(q,n_i,n_f)|^2, \quad (21)$$

where $E_z=E_{zf}-\hbar\omega_c(n_i-n_f)+\hbar\omega_{I\nu}\cdot\beta_\nu(q)$ and $M(q)$ are the e–IO–ph coupling function and the overlap integral, respectively.[9,10,12] The frequencies and relative functions describing the e–IO–ph coupling can be calculated similar to the previous paper.[12] An empirical interpolation effective-phonon-mode approximation (EPMA)[15,17] for TMC $\mathrm{Al}_x\mathrm{Ga}_{1-x}\mathrm{As}$ is used in constructing the IO-phonon modes in the system.[12,15] As was pointed out by previous works, there are eight branches of the IO-phonon modes coupling with the electrons in the whole DBS. The frequencies of the emitted IO phonons will be chosen as the corresponding values at the long-wavelength limit.[9]

In the above calculations we have not mentioned the LO_{cb}-PAMT current assisted by LO phonons confined in the collector barrier, since the electronic emission wave is rather

TABLE I. Parameters used in the numerical calculation. Energy is in units of meV and mass in units of the bare electrons (Ref. 15).

Quantities	GaAs	$Al_xGa_{1-x}As$
m^*	0.067	$0.067+0.083x$
$\hbar\omega_{LO}$	36.25	$36.25+1.83x+17.12x^2-5.11x^3$
$\hbar\omega_{TO}$	33.29	$33.29+10.70x+0.03x^2+0.86x^3$
ε_0	13.18	$13.18-3.12x$
ε_∞	10.89	$10.89-2.73x$

weak in the collector barrier so that the overlap integral M_m^{cb} is approximately zero and the corresponding current can be omitted.

III. NUMERICAL RESULTS AND DISCUSSION

We have performed the numerical calculations of the PAMT currents for the DBS GaAs/$Al_xGa_{1-x}As$ systems. The conduction-band offset is determined by $V(x)=750x$ (meV) for $x<0.45$ and $V(x)=750x+690(x-0.45)^2$ (meV) for $x\geqslant 0.45$.[19] The emitter and collector layers of the structures are both assumed to be n^+ doped at 2×10^{17} cm^{-3}, and Fermi level chosen as $E_F=20$ meV in the calculations. The temperature is determined as $T=4.2$ K, consistent with the corresponding experimental value.[2,3] Both the applied electric and magnetic fields and also the current are all assumed to be parallel to the z axis. Only the lowest-order Landau level in the emitter is considered, since depopulation of the higher-order levels occurs at a rather low magnetic field. The parameters used in the computation are listed in Table I and the results are illustrated in Figs. 1 and 2.

The PAMT current peaks have been experimentally observed[2,3] in the wider- and narrower-well cases, respectively. Only the first PAMT peak is easily observed when the well is wider, but the second peak appears as the well becomes narrower.[2] Our previous calculated results indicated[9,10] that the IO-PAMT current peak occurs at the voltage same as that of the well LO_w-phonon assisted peak and the two peaks merge each others, so that only one PAMT peak can be observed in the wider well case. To recognize theoretically the two-peak structure of the PAMT currents in the experiment results,[2,3] here we have calculated the contribution of the confined LO_{eb} phonons of the emitter barrier to the PAMT current in the narrower-well case, besides the IO- and well LO_w-phonon contributions. For ease of understanding the experiments we have chosen the DBS system that is the same as that observed by Leadbeater *et al.*,[2] i.e., the $Al_{0.4}Ga_{0.6}As/GaAs/Al_{0.4}Ga_{0.6}As$ system with the widths of 111 Å/58 Å/83 Å, at the magnetic field $B=11$ T, 6 T, 0 T, respectively.

In Fig. 1 we plot the curves of the PAMT currents assisted by the transitions from $n_i=0$ to $n_f=0$ and $n_f=1$ Landau levels. The PAMT current peak from $n_i=0$ to $n_f=0$ is found more important than that from $n_i=0$ to $n_f=1$. It is shown in Fig. 1(a) that the confined LO_w- and IO-PAMT current peaks occur at the same applied voltage $V=175$ mV, corresponding to the GaAs-like LO-phonon energy 36.25 meV, and the confined LO_{eb1}- and LO_{eb2}-PAT current peaks lie, respectively, at $V=194$ mV (with the phonon energy 46.32 meV) and $V=167$ mV (with the phonon energy 31.14 meV). The PAMT current peaks arrange from higher to lower as IO-, LO_{eb1}-, LO_w-, and LO_{eb2}-PAT peaks. Finally, the total PAMT current appears clearly two peaks, one of which is subjected to the mixture of the confined LO_w- and IO-PAMT currents corresponding to the bulk GaAs LO-phonon energy 36.25 meV, another is the confined LO_{eb1}-PAT current peak corresponding to the phonon energy of the AlAs-like modes 46.32 meV. The confined LO_{eb2}-PAT current peak corresponding to the phonon energy of GaAs-like modes 31.14 meV is submerged in the first peak. The phonon energy values corresponding to the calculated PAMT current peaks are in agreement with experimental results (35.5 and 48 meV).[2] In Fig. 1(b) a similar characteristic is seen at the lower magnetic field. Even the peaks of transition from $n_i=0$ to $n_f=1$ levels become higher, and the two peaks have blended together, with the magnetic filed is reduced to 6 T. However, Fig. 1(c) shown that the total PAMT current peak has a ''flat top'' structure at the magnetic field $B=0$ T. It is follows that the PAMT current peaks become higher and sharper and shift to the higher bias with increasing magnetic filed. Application of a higher magnetic field can resolve clearly the two distinct PAT peaks.

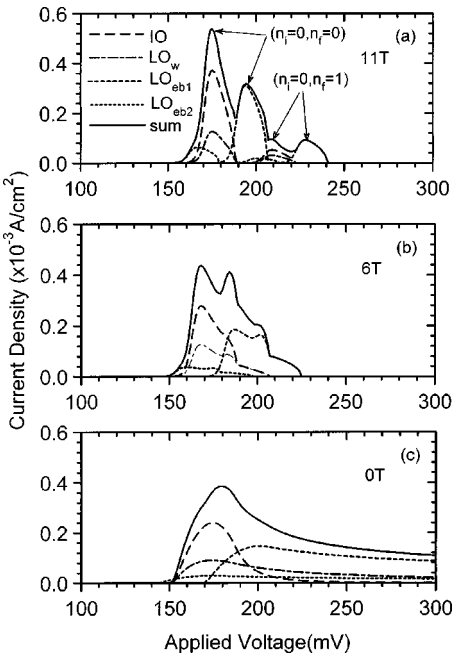

FIG. 1. The PAMT current densities as functions of the applied voltage V under various magnetic fields with narrower-well structure $Al_{0.4}Ga_{0.6}As/GaAs/Al_{0.4}Ga_{0.6}As$ with the widths of 111 Å/58 Å/83 Å for (a) 11 T, (b) 6 T, (c) 0 T.

The PAMT current densities as functions of the applied voltage V for the wider-well system corresponding to the situation in the experiment of Leadbeater *et al.*[2] are illustrated in Fig. 2. In the calculation, the structure has been chosen as $Al_{0.4}Ga_{0.6}As/GaAs/Al_{0.4}Ga_{0.6}As$ with the widths of 56 Å/117 Å/56 Å and the magnetic filed as $B=12$ T. It can

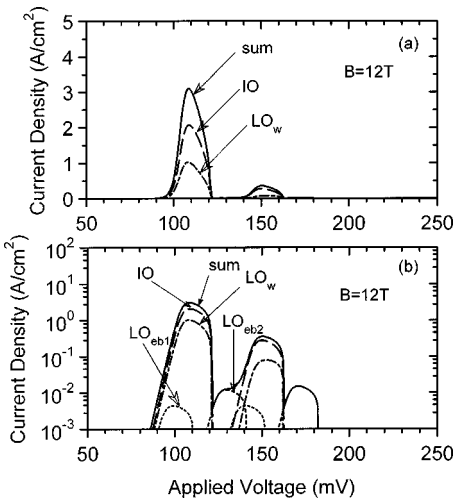

FIG. 2. The PAMT current densities as functions of the applied voltage V with wider well structure $Al_{0.4}Ga_{0.6}As/GaAs/Al_{0.4}Ga_{0.6}As$ with the widths of 56 Å /117 Å /56 Å at magnetic field $B=12$ T for (a) on a linear scale, (b) on a logarithmic scale.

be easy found that the PAMT current peaks from IO- and confined LO_w-phonons occur at the same voltage position corresponding to the GaAs-like LO-phonon energy 36.25 meV. The LO_{eb1}- and LO_{eb2}-PAMT currents are rather weak, so that cannot be easily observed. To clearly see the smaller PAT contributions, we plot the current densities in a logarithmic scale in Fig. 2(b). It can be seen that the confined LO_{eb1}- and LO_{eb2}-PAT currents are approximately two order of magnitude smaller than the IO- and LO_w-PAMT currents, because of the smaller overlap of the wave function in the emitter barrier. Therefore, only one PAMT current peak can be observed for the wider well systems.

We have also calculated the PAMT current peaks contributed, respectively, by the IO, the confined LO_w phonons (in the well) and the confined LO_{eb1} and LO_{eb2} phonons (in the emitter barrier) as functions of the well width d_3. It follows that only one PAT peak can be observed when the well is wider, but the second peak appears as the well becomes narrower. The conclusion is qualitatively similar to that in our previous work.[9] Different from Ref. 9, we have included here the two branches of LO-phonon modes in the TMC emitter barrier. The results indicate that the second peak is subjected to the LO_{eb1} phonons of the higher-frequency (AlAs-like) branch.

In our calculation, the PAT peak positions along the applied voltage axis do not agree with the experimental peaks[2] because the complication of the systems used in experiments. To focus attention on the recognition of PAT peaks we have adopted an ideal DBS model, by which calculated results for the phonon energies corresponding to the PAMT peaks agree with those in experiments. In order to completely fit the voltage scale (or, equivalently, PAT peaks lineshape), the complicated structure of the systems, charge trapping effect, electron-electron interaction, and plasmon-phonon coupling, etc, should be taken into account. These will be considered in the further works.

In summary, we have investigated the PAMT processes in $GaAs/Al_xGa_{1-x}As$ DBS including the two-mode behavior of TMC $Al_xGa_{1-x}As$ barriers. The contributions of the LO_{eb1}-, LO_{eb2}-, LO_w-, and IO phonons to the PAMT currents are analyzed in detail. An alternative recognition of optical PAMT peaks in $GaAs/Al_xGa_{1-x}As$ DBS is made by the numerical calculations. The results show that the IO- and LO_w-PAMT current peaks occur at the same voltage position, and are dominant and sole observable when the well of DBS is wider. The second peak corresponding to the emission of confined LO_{eb1} phonon in the emitter barrier can be observed only in the narrower-well systems. Our recognition of the PAMT peaks can explain qualitatively the related experimental phenomena.[2,3]

ACKNOWLEDGMENTS

The work was supported by the National Natural Science Foundation of China (Project 19764001) and the Natural Science Foundation of Inner Mongolia Autonomous Region of China (Project 20001301) and the 321 project of Inner Mongolia Autonomous Region of China. The authors wish to thank Professor S. L. Ban for helpful discussions.

*Email address: zwyan@imau.edu.cn
†Email address: xxliang@imu.edu.cn
‡Mailing address.

[1] V. J. Goldman, D. C. Tsui, and J. E. Gunningham, Phys. Rev. B **36**, 7635 (1987).
[2] M. L. Leadbeater, E. S. Alves, L. Eaves, M. Henini, O. H. Hughes, A. Celeste, J. C. Portal, G. Hill, and M. A. Pate, Phys. Rev. B **39**, 3438 (1989).
[3] G. S. Boebinger, A. F. J. Levi, S. Schmitt-Pink, A. Passner, L. N. Pfeiffer, and K. W. West, Phys. Rev. Lett. **65**, 235 (1990).
[4] N. S. Wingreen, K. W. Jacobsen, and J. W. Wilkins, Phys. Rev. B **40**, 11 834 (1989).
[5] F. Chevoir and B. Vinter, Appl. Phys. Lett. **55**, 1859 (1989).
[6] P. J. Turley and S. W. Testsworth, J. Appl. Phys. **72**, 2356 (1992).
[7] H. Zhou, Yuan-t Du, and T.-h. Lin, Phys. Rev. B **54**, 2691 (1996).
[8] P. Orellana, F. Claro, E. Anda, and S. Makler, Phys. Rev. B **53**, 12 967 (1996).
[9] Z. W. Yan, X. X. Liang, and S. L. Ban, Phys. Rev. B **64**, 125321 (2001).
[10] Z. W. Yan and X. X. Liang, J. Appl. Phys. **91**, 724 (2002).
[11] N. Mori and T. Ando, Phys. Rev. B **40**, 6175 (1989).
[12] Z. W. Yan and X. X. Liang, Int. J. Mod. Phys. B **15**, 3539 (2001).
[13] J. J. Licari and R. Evrard, Phys. Rev. B **15**, 2254 (1977).
[14] I. F. Chang and S. S. Mitra, Adv. Phys. **20**, 359 (1971).
[15] S. Adachi, J. Appl. Phys. **58**, R1 (1985).
[16] X. Wang and X. X. Liang, Phys. Rev. B **42**, 8915 (1990).
[17] X. X. Liang and J. S. Yang, Solid State Commun. **100**, 629 (1999).
[18] X. X. Liang and S. L. Ban, J. Lumin. **94–95**, 781 (2001).
[19] Y. Ando and T. Itoth, J. Appl. Phys. **61**, 1497 (1987).
[20] S. L. Ban, J. E. Hasbun, and X. X. Liang, J. Lumin. **87–89**, 369 (2000).